Transport properties of liquid alcohols investigated by IQENS, NMR and DLS studies

1996 J. Phys.: Condens. Matter 8 8157

(http://iopscience.iop.org/0953-8984/8/43/012)

J. Phys.: Condens. Matter **8** (1996) 8157–8171. Printed in the UK

Transport properties of liquid alcohols investigated by IQENS, NMR and DLS studies

M P Jannelli†, S Magazù†, P Migliardo†, F Aliotta‡ and E Tettamanti§

† Dipartimento di Fisica dell'Università and INFM, Università di Messina, PO Box 55, 98166 S Agata, Messina, Italy

‡ Istituto di Tecniche Spettroscopiche del CNR, 98166 S Agata (Messina), Italy

§ Dipartimento di Fisica dell'Università and INFM, Università dell'Aquila, 67010 Coppito, L'Aquila, Italy

Received 15 May 1996, in final form 7 August 1996

Abstract. We present new results, obtained by integrated application of different techniques (IQENS, NMR, DLS and viscosity measurements), on three alcohols, $[CH_3(CH_2)_nOH]$ ($n = 1, 7, 9$), namely ethanol, octanol and decanol. The revealed temperature dependence of the transport coefficients allows us to frame these H-bonded systems in the moderately strong Angell kinetic classification. The translational diffusion coefficient scales with the chain length, so suggesting that the diffusing entities do not present coiling effects. Furthermore, a *fast* and a *slow* rotational diffusive process have been identified. The former, revealed by both IQENS and DLS techniques, has been connected with the fast rotational jumping of the CH_3 group. The latter makes the evaluation of the static correlation factor possible, after a comparison of the neutron and the DLS data. Finally, the translational and reorientational dynamics of these H-bonded systems is discussed within the framework of the current theories.

1. Introduction

Many techniques are today available to probe the translational and rotational diffusive dynamics in molecular liquid systems. In comparing results from different techniques attention should be paid on the *self* or *collective* character probed [1–3]. It is a widely held view, for example, that incoherent quasi-elastic neutron scattering (IQENS) and nuclear magnetic resonance (NMR) give information on diffusive single-particle correlations [2–5], whereas dynamic light scattering (DLS), such as that of Rayleigh-wing type [6, 7], allows the cooperative nature of molecular diffusion to be tested for. It is clear that on this basis, a fruitful trend towards reaching a fairly accurate picture of the extent to which diffusion processes are cooperative requires the integrated application of different approaches.

In this paper we report results from NMR, QENS, and DLS techniques and viscosity measurements, on ethanol $[CH_3CH_2OH]$, octanol $[CH_3(CH_2)_7OH]$, and decanol $[CH_3(CH_2)_9OH]$. The present study is a part of an extensive analysis that we have carried out on hydrogenous systems and was performed to gain a better understanding of the diffusive properties of these systems, to determine the role played by the alcohol length, and to test for the occurrence of coiling effects.

In recent years, the study of the microscopic dynamics of hydrogen-bonded liquids has attracted a great deal of attention. It is commonly accepted that the existence of the highly directional H bond, whose energy value normally ranges between $\sim$8 kJ mol^{-1}

0953-8984/96/438157+15$19.50

and $\sim$25 kJ mol^{-1} [8], induces different chemical–physical properties and different local environments. As the mean lifetime of the H bond is in the ps time-scale, such structures are to be considered as *transient species* in dynamical equilibrium.

In the last few years, alcohols have been the focus of a number of studies but, although substantial progress has been achieved in the elucidation of their local short-range structure and single-particle dynamics, strong cooperative effects, caused by the existence of the hydrogen-bond network, are not fully explained. In particular the effects of the competitive mechanisms between their hydrophobic and hydrophilic parts and their variation with the alcohol length are still poorly understood. From this standpoint one would expect that hydrophilic effects are more pronounced in short alcohols and become less and less significant when the alcohol length increases. Owing to the difference between the lengths and to the degree of branching of the alkyl chains, in fact, these systems exhibit different aggregative properties. In particular Raman, IR, static dielectric and viscosity measurements indicate for the linear normal-pentanol (n-PeOH) the existence of oligomers with a zigzag structure [9–11]. It is to be expected that steric hindrance effects will increase with the chain length.

On the other hand, despite the relative wealth of the proposed models, the data interpretation, within idealized theoretical frameworks, may be quite difficult, because of the concomitant presence of different kinds of diffusional molecular processes. Therefore, from the experimental point of view, it seems nowadays clear that a proper analysis of the individual components, coming from different diffusing entities, and of possible cooperative effects should be taken into account. Given this, since decomposition into more than a few contributions may represent, in certain cases, a debated problem, because of the ill-conditioned nature of such an estimation, simplifying assumptions and the simultaneous use of different experimental techniques is strongly recommended. Finally, very few experimental works exist in the literature concerning with the integrated employment of NMR, IQENS and Rayleigh-wing light scattering for making possible the separation of the translational (by means of NMR and IQENS) and rotational (by IQENS and Rayleigh-wing light scattering) contributions as well as for providing evidence for the possible existence of cooperative phenomena.

The assumption of this study is that the joint employment of the three methodologies can furnish a complete reference picture for the comprehension of the diffusive properties of these H-bonded liquids, besides providing evidence of their dependence on the alcohol length.

2. The experimental set-up and data handling

High-purity samples of ethanol, octanol and decanol (certified grade quality products) were further purified, degassed and then filtered inside a dry box in order to remove dust particles and inhomogeneities, following a procedure described previously [12, 13].

Diffusion coefficient measurements were performed using the NMR pulsed spectrometer Bruker SX-P-4-100 MHz, working at a frequency of 85 MHz for the protons. The samples, contained in an NMR tube, with an inner diameter of 6 mm, were thermostated within 0.25 °C by means of an air-flow system, Bruker BT-1000. The measurements were performed over the temperature range 10–50 °C, with steps of 5 °C. The measurements were performed by means of the Hahn (see [14, 15]) spin-echo sequence, by varying the continuous gradient value G, so as to obtain a relaxation of about one decade for the echo signal as a function of gradient. From the fit of the logarithm of the amplitude signal echo versus G^2 the diffusion coefficient was determined. The signal was revealed by means

of an ADC Datalab DL 912 and averaged on line by a computer. The magnitude of the magnetic field gradient was calibrated, versus current, using a water sample and observing the echo signal that results modulated according to a Bessel function. From the time interval between minima and maxima of the modulated echo profile, we have determined the gradient strength. In the case of decanol the diffusion coefficient measurements were also performed with a rectangular magnetic field gradient as described by Stejskal and Tanner [16], using a pulse gradient unit, Bruker B-Z18B. The values obtained coincide with those evaluated by means of the continuous gradients.

The IQENS measurements were performed, at $T = 25\ ^{\circ}$C, with the MIBEMOL t.o.f. spectrometer at the ORPHEE reactor in Saclay. The neutron wavelength was 8 Å and the exchanged wavevector spanned the range $0.273\ \text{Å}^{-1} \leqslant Q \leqslant 1.456\ \text{Å}^{-1}$. The energy resolution (vanadium sample) was better than 20 μeV (HWHM). A high statistical accuracy was achieved ($\simeq$0.1% at peak maxima) by counting over large periods. The IQENS spectra were corrected for the empty-cell contribution, transformed to the energy scale and symmetrized for the detailed balance in the energy range spanned.

As far as the depolarized-light scattering measurements are concerned the samples were sealed in optical rectangular silica cell of size $10 \times 10 \times 80$ mm and then mounted in an optical thermostat especially built to avoid any unwanted stray-light contributions. The measurements were performed at $T = 25\ ^{\circ}$C with a temperature stability better than 0.05 °C. The high purity of the samples, as well as the optical purity of the sample holder, ensured collection of data with a good signal-to-noise ratio and with high reproducibility. We used, in a 90° scattering geometry, a high-resolution fully computerized Spex-Ramalog triple monochromator. As the exciting source, the 4880 Å vertically polarized line of a unimode Ar^+ laser, Spectra Physics Model 165, working at a mean power of 700 mW was used. The detection apparatus consisted of a photon-counting system, whose outputs were processed on line by a computer. The depolarized scattered intensity was automatically normalized for the incoming beam intensity. Following a well established procedure, described previously [17], spectral resolutions of $0.10 \pm 0.05\ \text{cm}^{-1}$ (HWHM) in the -3 to 3 cm^{-1} region, of 0.25 cm^{-1} in the $-8\ \text{cm}^{-1}$ to 8 cm^{-1} region, and of 1.5 cm^{-1} in the -100 to 400 cm^{-1} region were used. The spectra at different resolutions were subsequently numerically matched and corrected for the density ρ, for the refractive index n and for local field effects [18–20]. These corrections correspond to a normalization of the intensity with the factor $n\rho^{-1}(n^2+2)^{-4}$, with n and ρ taken from literature [21]. Finally the Stokes and anti-Stokes sides of the spectra were properly normalized by means of the 'detailed-balance' law. The extracted linewidths were reproducible to better than 5%.

For the auxiliary viscosity measurements, standard Ubbelohde viscometers, mounted in a suitable thermostat bath which stabilizes temperature within $\pm 0.02\ ^{\circ}$C, were employed. The viscometers were chosen with long flow times in order to minimize the kinetic energy correction. Experimental data turn out to be reproducible with an indeterminacy lower than one part per thousand.

3. Results and discussion

3.1. NMR and viscosity data

It is well known that the self-diffusion coefficient D_T represents the zero-frequency limit of the Fourier transform, $\phi(\omega)$, of the centre-of-mass velocity autocorrelation function:

$$D_T = \frac{\pi k_B T}{m} \lim_{\omega \to 0} \phi(\omega) \tag{1}$$

where k_B is Boltzmann's constant, T is Kelvin's absolute temperature and m is the mass of the diffusing entity.

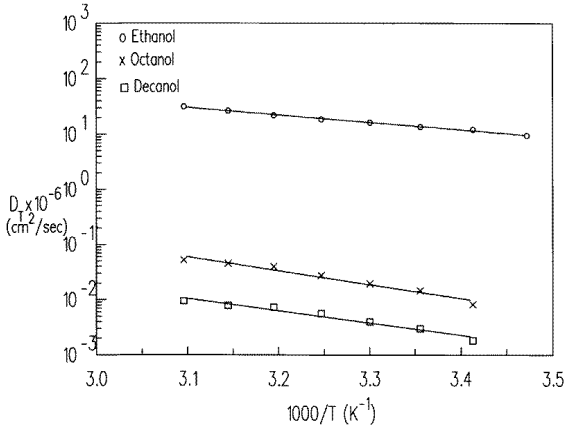

Figure 1. Translational diffusion coefficients D_T, obtained from NMR data, as functions of the temperature for ethanol (○), octanol (+) and decanol (□). The continuous lines are the fit results.

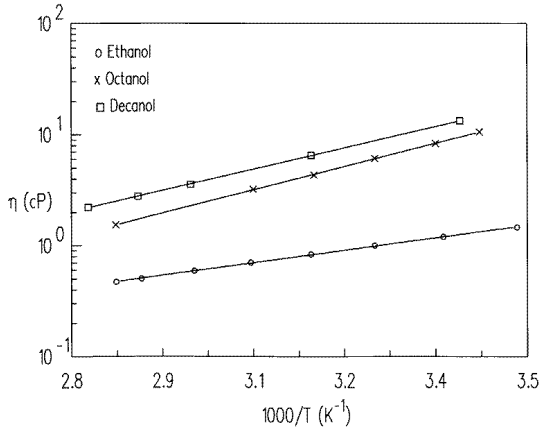

Figure 2. An Arrhenius plot of shear viscosity for ethanol (○), octanol (+) and decanol (□). The continuous lines are the fits.

Provided that a single kinetic process drives the translational diffusive motions and the viscous flow, and assuming the Stokes–Einstein relationship between the translational self-diffusion coefficient and viscosity, a common activation energy E is expected, namely:

$$D_T \propto T/\eta \propto \exp(-E/RT). \tag{2}$$

This relation implies that the ratio $D_T\eta/T$ keeps constant as temperature changes. In our case, as will be shown below, in the temperature range investigated such a relationship is not very well satisfied, indicating that a simple law for diffusion cannot be applied for alcohols.

In figure 1 the behaviours of the translational self-diffusion coefficients D_T for ethanol, octanol and decanol are reported in an Arrhenius plot. As can be seen, D_T increases linearly with temperature, furnishing activation energy values of 12.83 kJ mol^{-1}, 21.23 kJ mol^{-1} and 24.16 kJ mol^{-1}, for ethanol, octanol and decanol respectively. In addition, as expected, D_T shows a decrease with the alcohol chain length. By applying a bond lattice model, in which an associated liquid can be pictured as an ensemble of *intact* and *broken* bonds (states *on* and *off*), the values obtained indicate that, when the chain length increases, the transition between the two kinetically allowed states becomes more difficult and the self-diffusive dynamics slower.

Concerning the temperature dependence of shear viscosity, the Arrhenius-like phenomenological law is, as shown in figure 2, again fulfilled [22]. As is well known, according to Kauzmann and Eyring [23], the macroscopic viscosity of a Newtonian liquid can be expressed in terms of its activation parameters by the relation

$$\eta \sim \phi \exp(\Delta H_\eta / RT) \exp(-\Delta S_\eta / R) \tag{3}$$

where ϕ is the molar volume of the liquid, ΔH_η is the activation energy per mole, ΔS_η is the corresponding entropy of activation and R is the gas constant. Since in a moderate range of temperature ϕ and ΔS_η do not vary very much, the above equation can be simplified into the two-parameter form suggested by Arrhenius:

$$\eta = A \exp(\Delta H_\eta / RT) \tag{4}$$

where the pre-exponential term A corresponds to the viscosity at infinite temperature.

In our case, over the temperature range investigated, the Arrhenius least-squares fit of the experimental data furnishes activation energies for the viscous flow of $\sim$7.23 kJ mol^{-1}, $\sim$13.45 kJ mol^{-1} and $\sim$12.33 kJ mol^{-1} for ethanol, octanol and decanol respectively. These values, lower than those found for the translational self-diffusion, support the assumption that a common, *but not unique*, thermally activated process, namely the breaking and reforming of the intermolecular H bond, drives both the translational diffusive motions and the viscous flow. We can hypothesize that the fundamental diffusion process depends upon the conditions necessary for a *normal* diffusion as well as upon the percentage of broken bonds, this latter being connected with the fraction of the diffusing species in the network. It is well known, in fact, that in the liquid phases of alcohols, either neat or dissolved in inert solvent, a percentage of labile clusters (molecules linked by hydrogen bonds between their hydroxyl group and the oxygen electronic lone pair of a nearest neighbour) exist. As a consequence the overall diffusion rate should be dependent on both of these factors. It should also be pointed out that a better agreement with equation (2) should be obtained by replacing η with the system microviscosity.

On the other hand the peculiar Arrhenius trend of these transport parameters allows us to frame our H-bonded systems within Angell's classification of strong and fragile liquids [24–27]. As is well known, liquids in the strong class change their viscosity with temperature in an almost Arrhenius fashion, exhibiting only a single relaxation time. In fragile liquids viscosity changes in a more complex way, exhibiting regions of non-Arrhenius character. This classification is named η_s-based to distinguish it by the ΔC_p-based one. Following this latter, a liquid is classified as fragile (strong) if a large (small) variation in heat capacity ΔC_p, on crossing T_g, occurs. These classifications are strictly connected to the number of configurations that the liquid can assume when temperature is changed and to the height of the energy barriers between them. While hydrogen-bonded liquids, like our alcohols, appear exceptionally fragile when framed in the ΔC_p-based classification, they look like intermediate liquids when considered from the η_s-based point of view. This circumstance

can be rationalized if, besides a high density of configurational states, one takes into account high energy barriers between adjacent configurational states, connected with the occurrence that the breaking of a proportion of hydrogen bonds is required to allow a configurational rearrangement. From this viewpoint, our three alcohols, in the temperature ranges investigated, show a moderately strong kinetic character.

3.2. IQENS data

Incoherent quasi-elastic neutron scattering [4], due to the space-time scale to which it is sensitive and to the simplification brought about by the weak neutron–nucleus interaction, meets very well the necessary requirements for the investigation of the translational and rotational diffusive processes in liquids of small molecules. In addition, the unique neutron isotope sensitivity allows us in many cases to select an incoherent or coherent nature for the scattering.

It is well known that the measured incoherent dynamical structure factor, $S_{inc}(Q,\omega)$, represents the double Fourier transform of the self part of the van Hove space-time correlation function $G_{self}(r,t)$.

The first problem occurring in the analysis of the IQENS spectra is concerned with the number of components contributing to the observed intensity. So far, there is no generally accepted agreement about the correct approach to this question. In this work, we started our analysis procedure by estimating the minimum number of Lorentzians required to reproduce the spectrum. According to Sears' formalism [4], which assumes a decoupling of the translational and rotational motions as well as uncorrelated rotational motions, our experimental spectra should be fitted with the following scattering law [4, 27, 28]:

$$S_s(Q,\omega) = \mathrm{e}^{-Q^2\langle u^2\rangle/3}\left\{J_0^2(Qa)\frac{1}{\pi}\frac{\Gamma_T}{(\Gamma_T)^2+\omega^2} + \sum_{l=1}^{\infty}(2l+1)J_l^2(Qa)\frac{1}{\pi}\frac{\Gamma_T + l(l+1)D_r}{[\Gamma_T + l(l+1)D_r]^2+\omega^2}\right\} \tag{5}$$

where J_l are the Bessel spherical functions, D_r is the rotational diffusion coefficient, Γ_T is the translational linewidth and the other symbols have the usual meanings.

In fact our fitting procedure was able to resolve just three independent Lorentzian lines, after convolution of the scattering law with the instrumental resolution function:

$$S_s(Q,\omega) = \mathrm{e}^{-Q^2\langle u^2\rangle/3}[L_1(Q,\omega) + L_2(Q,\omega) + L_3(Q,\omega)] \otimes R(Q,\omega) \tag{6}$$

where $L_i(Q,\omega)$ are Lorentzian lines and $R(Q,\omega)$ represents the resolution obtained with a standard vanadium sample. The first Lorentzian exhibits a markedly Q-dependent linewidth, whereas the other two show a Q-independent broadening.

Although such assumptions could appear rather simplifying for the class of fluids that we are dealing with, they give a tractable form which allows us to separate the different dynamical processes; in addition, most of the works previously reported for such systems have been carried out along the same lines. On the basis of the usually accepted interpretation developed in earlier IQENS studies on H-bonded systems [25–28], the three spectral Lorentzian contributions have been assigned to the following three different motions: a centre-of-mass motion, associated with the Q-dependent Lorentzian contribution, a spherical rotational tumbling of the molecule as a whole, associated with the slow Lorentzian contribution, and a fast rotation of the methyl group relative to the C–O axis, associated with the faster one.

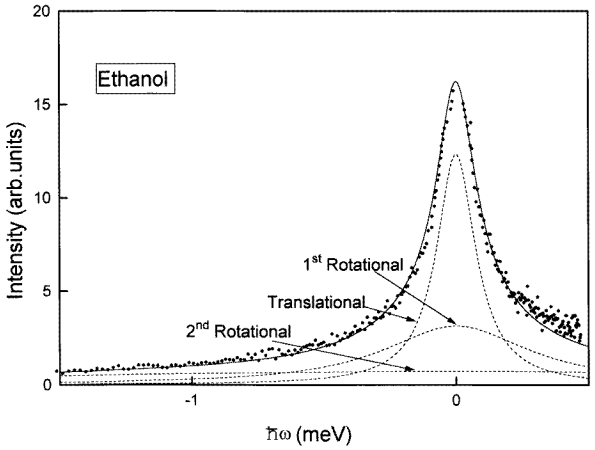

Figure 3. The IQENS spectrum for ethanol, at $Q = 0.98$ Å^{-1}. Points: experimental data; continuous line: fit result with equation (6); dashed lines: Lorentzian components (see the text for details).

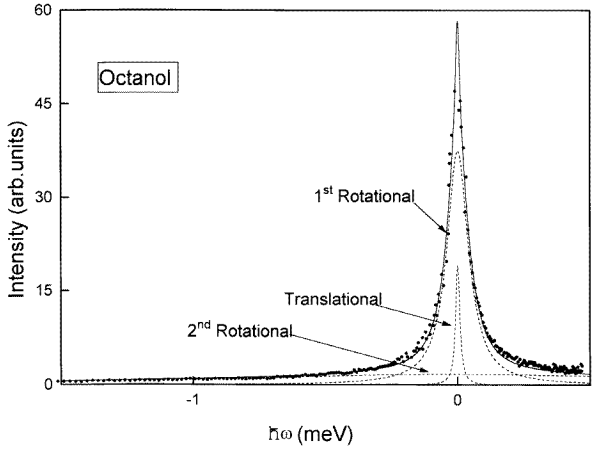

Figure 4. The IQENS spectrum for octanol, at $Q = 0.98$ Å^{-1}. Points: experimental data; continuous line: fit result with equation (6); dashed lines: Lorentzian components (see the text for details).

Figures 3, 4 and 5 show, as an example, the experimental data, at $T = 25$ °C, and the fit results together with the decomposition of the lineshapes into the different spectral contributions, namely the translational and the two rotational components, for ethanol, octanol and decanol respectively. The relevant IQENS parameters, as obtained by the fitting procedures, are reported in table 1 together with the NMR data for the translational diffusion parameters, taken at $T = 25$ °C, and the Rayleigh-wing data at the same temperature which will be discussed in the following.

As far as the translational contribution of the IQENS data is concerned, the dependence of the quasi-elastic linewidth (HWHM), Γ_T, as a function of Q^2, in the Q-range investigated, follows a linear behaviour for the three alcohols—see figure 6—closely resembling the linear

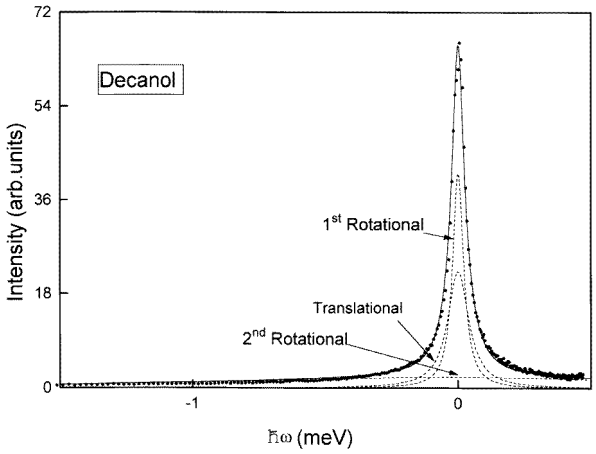

Figure 5. The IQENS spectrum for decanol, at $Q = 0.98$ Å^{-1}. Points: experimental data; continuous line: fit result with equation (6); dashed lines: Lorentzian components (see the text for details).

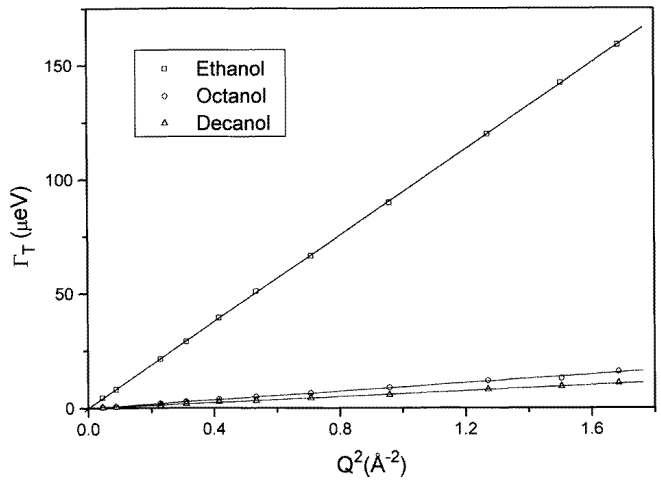

Figure 6. The translational linewidth (HWHM) Γ_T versus Q^2, for ethanol (□), octanol (○) and decanol (△). The continuous line represents the linear best fit.

$D_T Q^2$-trend, predicted by the hydrodynamic theory. From the values of $\Gamma_T(Q)$ we have derived the translational diffusion coefficients, D_T, which are in excellent agreement with the ones obtained by NMR.

As far as the linear behaviour of Γ_T versus Q^2 is concerned, a different model, kinetic in character, has been developed by Bertolini *et al* [29] and successfully applied by Bermejo *et al* [30] for liquid methanol, and by Migliardo [27] for isomeric pentanols. In summary this model furnishes an intermediate scattering function for the translational diffusion:

$$F_s^{Total}(Q,t) = \sum_{i=0}^{2} f_{S,i} F_{S,i}^{T}(Q,t) \tag{7}$$

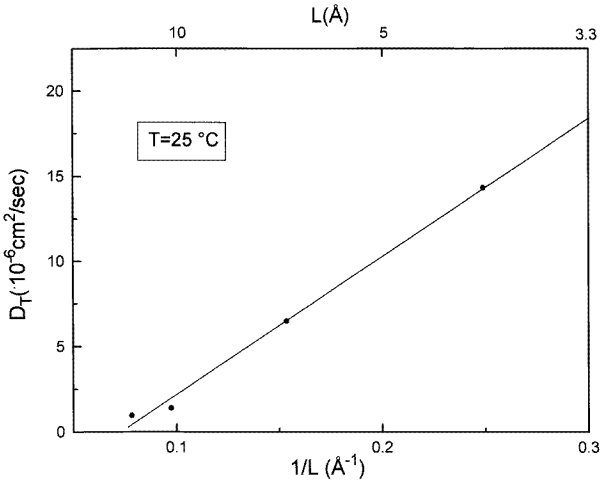

Figure 7. The behaviour of the translational diffusion coefficient D_T (obtained from IQENS data) versus the inverse chain length $1/L$.

Table 1. Translational diffusion coefficients, obtained from NMR and IQENS data, and rotational times, obtained from IQENS and Rayleigh-wing data, for ethanol, octanol and decanol. $T = 25\ ^\circ$C.

	$D_T \times 10^{-6}$ (cm^2 s^{-1})		τ_R (ps)		$\tau_R(CH_3)$ (ps)	
	NMR	IQENS	IQENS	Rayleigh wing	IQENS	Rayleigh wing
CH_2CH_3OH	14.423	14.338	1.95	5.86	0.3	0.26
$CH_2(CH_3)_7OH$	1.443	1.405	13.44	33.49	0.3	0.26
$CH_2(CH_3)_9OH$	0.96	0.97	25.33	40.78	0.3	0.26

where the $f_{S,i}$ are the percentages of the 0, 1, 2 *intact* bonds to which self-diffusion coefficients D_i correspond. The total diffusion coefficient results:

$$D_T = \sum_{i=0}^{2} f_i D_T^i. \tag{8}$$

When $Q \neq 0$ the bond dynamics becomes comparable with the translational dynamics and the resulting D_T becomes a function of the various diffusion coefficients as well as of the parameters that drive the H-bond dynamics. Unfortunately, in our case the percentage of intact bonds $f_{S,i}$ is not known and such an evaluation cannot be performed. Anyway, the close correspondence between the NMR and IQENS D_T-data is a convincing argument that our determination is concerned with the translational diffusional value weighted over the different inherent structures, rendering knowledge of the various D_T^i inessential.

Finally, by comparing the self-translational-diffusion coefficients we do not find a dynamical scaling relation with the inverse cubic root of molecular weight M, namely $D_T \sim M^{-1/3}$, as predicted by the Stokes–Einstein relationship in the case of spherical diffusing entities [31]. This transport coefficient, instead—see figure 7—is found to be inversely proportional to the alcohol chain length L, calculated from the values of bond lengths and the bond angles assuming cylindrical molecules. In the same figure the self-diffusion coefficient of normal pentanol, $[CH_3(CH_2)_4OH]$, measured in a previous study

[27], is also reported. As can be seen, the data arrange themselves along a straight line so suggesting that coiling effects are not present, probably because of the small length of the chain.

As far as the rotational dynamics of our H-bond systems is concerned, the two rotational neutron relaxation times, obtained as parameters of the Q-independent contributions and reported in table 1, suggest the existence of a rather slow tumbling of the alcohol molecules due to coupling to the dynamics of the hydrogen-bond network, and a second fast rotational mode arising from the internal reorientation of the methyl group [30, 32]. In the following, a comparison with the rotational relaxation times obtained by means of light scattering is presented.

3.3. DLS data

It is well known that depolarized Rayleigh scattering in a liquid system is originated by the time correlation $C_\beta^{anis}(Q,t)$ of the traceless part of the polarizability tensor fluctuations $\delta\beta_{ij}(Q,t)$ [6]. Usually, both the permanent and the induced contributions of this latter enter in the $C_\beta^{anis}(Q,t)$. The Rayleigh-wing intensity, $I_{VH}(Q,\omega)$, defined as the Fourier transform of $C_\beta^{anis}(Q,t)$, can be written in the form

$$I_{VH}(Q,\omega) = \int_{-\infty}^{\infty} \mathrm{d}t \exp[-\mathrm{i}\omega t] \left\{ \langle \delta\beta_{xy}^*(Q,0)\delta\beta_{xy}(Q,t)\rangle \sin^2\frac{\vartheta}{2} + \langle \delta\beta_{yz}^*(Q,0)\delta\beta_{yz}(Q,t)\rangle \cos^2\frac{\vartheta}{2} \right\} \tag{9}$$

where $\langle\ \rangle$ denotes the thermodynamical averaging, θ is the scattering angle and for the scattering geometry we refer the reader to reference [6]. $\delta\beta_{ij}(Q,t)$ also takes into account the translational term

$$\delta\beta_{ij}(t) = \frac{1}{V}\sum_\alpha \delta\beta_{ij}^{(\alpha)}(t)\exp[-\mathrm{i}Qr_\alpha(t)]. \tag{10}$$

$I_{VH}(Q,w)$ contains both the self and the distinct contributions of the correlation function $C_\beta^{anis}(Q,t)$. In other words, depolarized Rayleigh spectra depend on both self particle motions and correlated motions of different molecules. In H-bonded liquids, these latter contributions may become important and, as will be shown in the following, under certain assumptions, a relation between the self and the distinct relaxation times can be formulated. The effective anisotropic polarizability, $\delta\beta_{ij}$, takes into account the 'bore' molecular polarizability plus an interaction-induced contribution that will be reflected in the reorientational pair correlation function and into a DID (dipole–induced-dipole) term. The above-described effects give rise to a CILS contribution (collision-induced light scattering) for the DID term in the far wing and reorientational contributions in the narrow wing [5, 7, 33]. From a general viewpoint, low-frequency depolarized-light scattering can be determined by molecular reorientations, by internal rotation motions of end groups or of unhindered side groups, by segmental movements induced by some intrinsic flexibility, as well as by collision-induced effects and by orientational pair correlations (OPC) [32, 34–36].

The distortion of the molecular electronic distributions, originated by collision dynamics, will contribute to the spectra through a frequency-dependent term:

$$I^{CILS}(\omega) = F(\omega)\exp(-\omega/\omega_0) \tag{11}$$

where $F(\omega)$ is a slowly varying function, and the inverse of ω_0 is taken as a measure of the duration of a collision. In effect, Wang and Wright [37] pointed out that 'an exponential

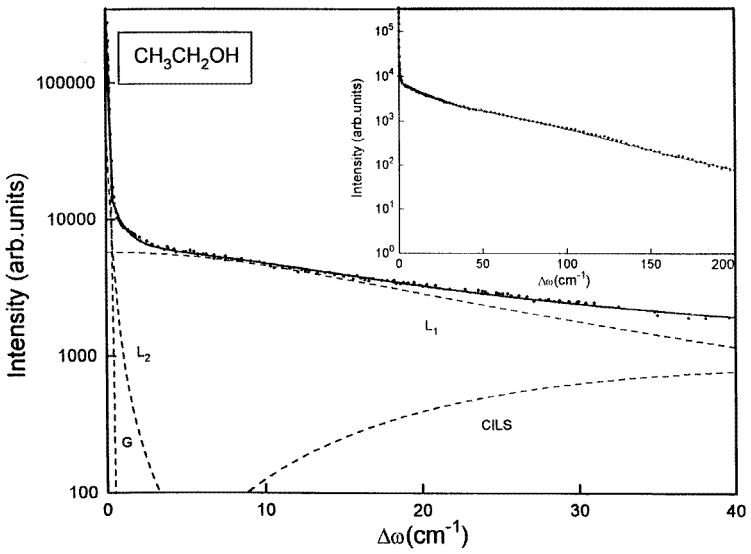

Figure 8. A semi-log plot of the experimental Rayleigh-wing spectrum, for ethanol at $T = 25$ °C. The continuous line represents the fit result, L_1 and L_2 are the two Lorentzian components, G is the Gaussian resolution function and CILS represents the collision-induced contribution. In the inset the experimental far-wing region of the spectrum (points) is shown, together with the best fit (continuous line).

shape cannot be considered as a criterion for collision-induced scattering'. As an example, in the case of monohydric alcohols, the ω_0^{-1}-value could be connected to the average period of the hydrogen-bond vibration of the aggregated species.

Bucaro and Litovitz [33], under the assumption of a total induced polarizability resulting from electron overlapping effects, in *head-on* binary collisions, and taking into account the molecular frame distortion, obtained, for the collision-induced scattering, the expression $F(\omega) = \omega^{2(m-7)/7}$. In particular, for molecular liquids, this gives the result $m = 13$, that, if one assumes a Lennard-Jones potential, would indicate an induced anisotropy originated by repulsive interactions. In our case, the fitting procedure performed furnishes for ω_0 the values of 22 cm^{-1}, 18 cm^{-1} and 16 cm^{-1} for ethanol, octanol and decanol, respectively. The value of ω_0 for ethanol is in good agreement with that obtained by Bucaro and Litovitz in their fit of the far wing with the CILS term. The trend of ω_0 is in agreement with the slowing down of the diffusional dynamics as the molecular weight of the diffusing entities increases [33, 37].

As far as the reorientational contributions are concerned, which are mainly of interest for the narrow-wing spectral region, different types of motion are expected to have different chain length dependences. Thus, the reorientation of the entire alcohol molecule should become significantly slower as the alcohol chain length increases, although the effects on simple end groups, as well as on eventual unhindered side chains, should be small; in addition, if relatively strong intermolecular forces (e.g. hydrogen bonding) are present, cooperative effects could be fairly large and should depend on the percentage of hydrophilic and hydrophobic parts of the alcohol chain. Finally, in our case, local backbone segmental motions are expected to show little change with molecular weight.

Egelstaff [1], in a very efficacious way, indicates how to compare IQENS and Rayleigh-

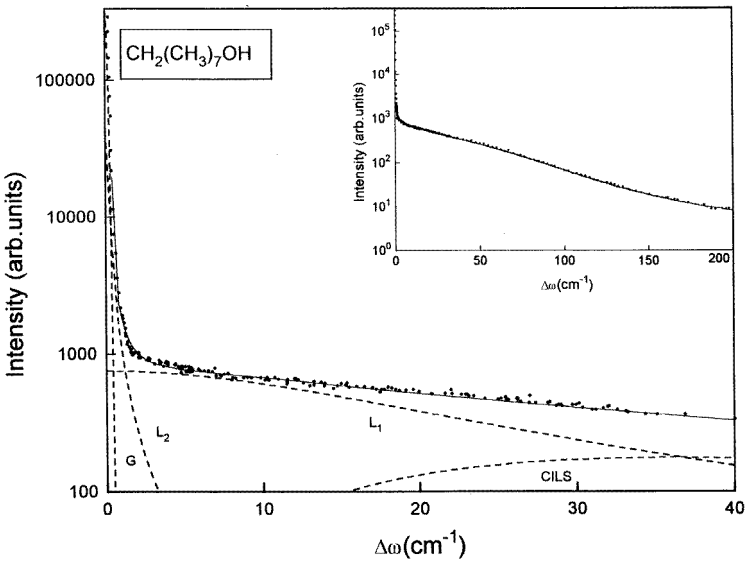

Figure 9. A semi-log plot of the experimental Rayleigh-wing spectrum, for octanol at $T = 25$ °C. The continuous line represents the fit result, L_1 and L_2 are the two Lorentzian components, G is the Gaussian resolution function and CILS represents the collision-induced contribution. In the inset the experimental far-wing region of the spectrum (points) is shown, together with the best fit (continuous line).

wing data. His method appears to be particularly fruitful for hydrogenous systems, in view of the incoherent nature of the proton cross-section. More precisely, under the assumption of no coupling between rotational and collective hydrodynamic modes, the microscopic–macroscopic correlation correspondence (CMMC) theorem [38, 39] ensures that, if the self rotational correlation function relaxes exponentially with a decay time τ_s, then also the OPC function is exponential, with a decay time proportional to τ_c. In formal terms the OPC time fulfils the simple expression

$$\tau_c = \tau_s[(1 + Nf)/(1 + Ng)] \tag{12}$$

where N is the number of the scatterers in the scattering volume, and f and g are the static and dynamic orientational correlation parameters [38]. These are defined as the normalized correlation functions of the second Legendre polynomials and their time derivatives respectively. The quantities $g_2 = (1 + Nf)$ and $J_2 = (1 + Ng)$ are named the static and dynamic correlation factors. Note that, if there are no correlations between different molecules, g_2 and J_2 are equal to unity. It is usually assumed, and this was tested for many liquids, that g is small enough (small time correlations between angular momenta of different molecules) to give $Ng \ll 1$. As a consequence one obtains

$$\tau_c = \tau_s(1 + Nf). \tag{13}$$

The experimental Rayleigh-wing data were fitted in terms of two Lorentzian lines, henceforth referred to as *fast* and *slow*, $L_1(\omega)$ and $L_2(\omega)$, a collision-induced contribution, $I^{CILS}(\omega)$, an *ultranarrow* resolution-enlarged Gaussian component, $G(\omega)$, and a small flat background contribution. In formal terms:

$$I_{VH}(\omega) = G(\omega) + L_1(\omega) + L_2(\omega) + I^{CILS}(\omega) + B. \tag{14}$$

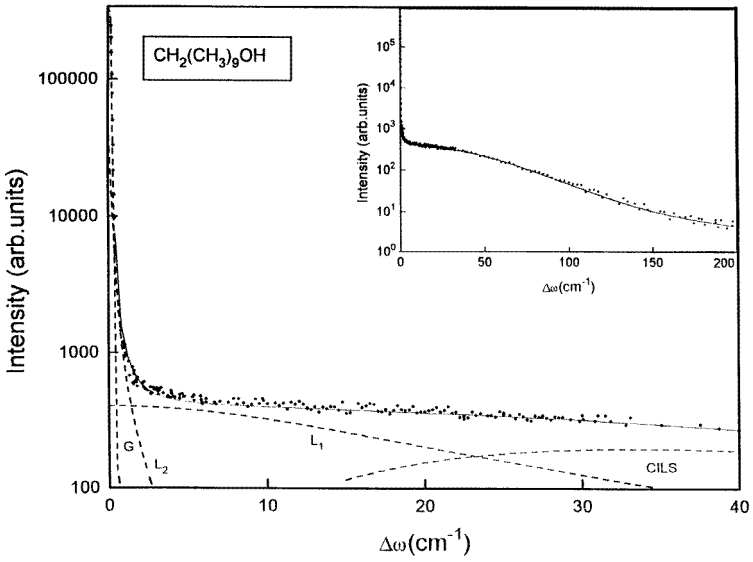

Figure 10. A semi-log plot of the experimental Rayleigh-wing spectrum, for decanol at $T = 25$ °C. The continuous line represents the fit result, L_1 and L_2 are the two Lorentzian components, G is the Gaussian resolution function and CILS represents the collision-induced contribution. In the inset the experimental far-wing region of the spectrum (points) is shown, together with the best fit (continuous line).

In figures 8, 9 and 10 we show Rayleigh-wing spectra for the three alcohols in a semi-log plot in the narrow region (0–40 cm^{-1}) together with the spectral components and the resulting fits. In the inset the experimental scattered intensities and the total fits are shown in the far spectral range examined (0–200 cm^{-1}). These spectral contributions provide good fits for each of the three alcohols, without invoking a sum of exponential functions in the ω-domain, as reported in reference [40], whose physical meaning cannot be clearly recovered. Each Lorentzian line furnishes a relaxation time $\tau = 1/2\pi\Gamma c$ (Γ being the HWHM linewidth). This analysis clearly shows that we are in presence of two distinct contributions [30, 32].

(i) The fast Rayleigh-wing relaxation times are almost independent of the nature of the alcohols and ultimately coincide, within the experimental uncertainties, with the neutron times. These results could indicate that we are observing an ultrafast jump of the non-interactive methyl groups, with mean time value of about 0.3 ps.

(ii) The slow Rayleigh-wing relaxation times have been assigned to the rotational tumbling of the molecules as a whole. These relaxation times turn out to be alcohol-type dependent and are noticeably higher with respect to the neutron ones, so indicating that the rotational diffusion has a cooperative character.

More precisely, we get the following results:

ethanol: $\tau_R^{Ray}/\tau_R^{neu} = \tau_c/\tau_s = g_2 = 3.01$

octanol: $\tau_R^{Ray}/\tau_R^{neu} = \tau_c/\tau_s = g_2 = 2.49$

decanol: $\tau_R^{Ray}/\tau_R^{neu} = \tau_c/\tau_s = g_2 = 1.61.$

The most noteworthy feature is that g_2 decreases in passing from ethanol to decanol as a

consequence of the competitive mechanisms between the hydrophobic part, which increases with the alcohol chain length, and hydrophilic part, not changing within the systems examined. This result indicates that hydrophilic effects are more pronounced in the shortest alcohol, where the intermolecular H bonds give rise to a greater degree of cooperative character, and become less and less significant when the alcohol length increases.

4. Concluding remarks

In this paper NMR, IQENS, light scattering and viscosity data on liquid alcohols are presented. The main points that emerge from experimental data are as follows.

(i) As far as the translational diffusion is concerned, the temperature evolution of the self-diffusion coefficients D_T, obtained by NMR and IQENS, behaves as many other physical quantities, for example shear viscosity. These behaviours suggest that a common, but not unique, process, namely the making and breaking of the intermolecular H bonds, can trigger both the translational diffusive motions and the viscous flow. In addition, the percentage of broken bonds, giving rise to different diffusing species, also drives slightly different rates for the translational diffusion process and the viscous flow. The temperature behaviour of the two transport coefficients allows us to frame the three alcohols investigated in the moderately strong Angell kinetic classification.

(ii) For the three alcohols, the dependence of the quasi-elastic neutron linewidth on the squared exchanged momentum follows the linear behaviour predicted by the hydrodynamic theory for continuous diffusion. Furthermore, the self-translational-diffusion coefficient is found to be inversely proportional to the alcohol chain length, so suggesting that the diffusing entities diffuse as cylindrical units with no evidence of coiling effects.

(iii) Regarding the rotational diffusive motions, two processes are identified by IQENS and Rayleigh-wing data. The first process has been connected with the fast rotational jumping of the methyl group; the second one, which has been attributed to the reorientation of the molecule as a whole, indicates that cooperative effects are present in our associated liquids. In addition, the comparison of the IQENS and Rayleigh-wing data made the evaluation of the static correlation factor possible. This latter parameter shows a decrease in passing from ethanol to decanol, suggesting that hydrophilic effects are more pronounced in the shortest alcohol, where the intermolecular H bonds give rise to a greater degree of cooperative character.

(iv) The far-wing Rayleigh spectra reveal the presence of a collisional contribution and allow one to evaluate the collision time. Its trend, as a function of the alcohol chain length, agrees with a slowing down of the diffusive dynamics due to heavier diffusing entities.

In summary, it was the integrated application of different spectroscopic techniques that allowed us to derive a more understandable picture of the dynamical responses of systems dominated by hydrogen-bond interactions, such as our alcohols.

References

[1] Egelstaff P A 1970 *J. Chem. Phys.* **53** 2590
[2] Kivelson D 1987 *Rotational Dynamics of Small and Macromolecules (Springer Lectures Notes in Physics 293)* ed T Dorfmuller and R Pecora (Berlin: Springer) p 1
[3] Dorfmuller T 1987 *Rotational Dynamics of Small and Macromolecules (Springer Lectures Notes in Physics 293)* ed T Dorfmuller and R Pecora (Berlin: Springer) p 65
[4] Bee M 1988 *Quasielastic Neutron Scattering* (Bristol: Hilger)

[5] Clarke J H R 1978 *Advances in Infrared and Raman Spectroscopy* vol 4, ed R J H Clark and R E Hester (London: Heyden) p 109
[6] Berne B J and Pecora R 1976 *Dynamic Light Scattering* (New York: Wiley)
[7] James D W 1985 *Advances in Infrared and Raman Spectroscopy* vol 12, ed R J H Clark and R E Hester (London: Heyden) p 311
[8] Angell C A *Water: A Comprehensive Treatise* vol 7, ed F Franks (New York: Plenum) pp 1–81
See also:
Schuster P, Zundel G and Sandorfy C 1976 *The Hydrogen Bond* vols I, II, III (Amsterdam: North-Holland)
[9] D'Aprano A, Donato D I, Migliardo P, Aliotta F and Vasi C 1988 *Phys. Chem.* **17** 279
[10] Magazù S, Majolino D, Mallamace F, Migliardo P, Aliotta F, Vasi C, D'Aprano A and Donato D I 1989 *Mol. Phys.* **66** 819
[11] Magini M, Paschina G and Picculuga G 1982 *J. Chem. Phys.* **77** 2051
[12] D'Aprano A, Donato D I, D'Arrigo G, Bertolini D, Cassettari M and Salvetti G 1985 *Mol. Phys.* **55** 475
[13] D'Aprano A, Donato D I, Migliardo P, Aliotta F and Vasi C 1988 *Phys. Chem. Liq.* **17** 279
[14] Hahn E L 1950 *Phys. Rev.* **80** 580
[15] Carr H Y and Purcell E M 1954 *Phys. Rev.* **94** 630
[16] Stejskal E O and Tanner J E 1965 *J. Chem. Phys.* **42** 288
[17] Aliotta F, Vasi C, Maisano G, Majolino D, Mallamace F and Migliardo P 1986 *J. Chem. Phys.* **84** 4731
[18] D'Arrigo G, Maisano G, Mallamace F, Migliardo P and Wanderlingh F 1981 *J. Chem. Phys.* **75** 4264
[19] Eckardt G and Wagner W G 1966 *Mol. Spectrosc.* **19** 407
[20] Burham A K, Alms G R and Flygare W H 1975 *J. Chem. Phys.* **62** 3289
[21] D'Aprano A, Donato D I and Agrigento V 1981 *J. Solution Chem.* **10** 673
[22] Arrhenius S 1916 *Medd. Vetensk. Nobel* **3** 20
[23] Kauzmann W and Eyring H 1940 *J. Am. Chem. Soc.* **62** 3113
[24] Angell C A 1984 *Relaxation in Complex Systems* ed K L Ngai and G B Write (Washington, DC: National Technical Information Service, US Department of Commerce) pp 3–11
[25] Angell C A 1991 *Hydrogen-Bonded Liquids (NATO-ASI Series)* vol 329 (Dordrecht: Kluwer Academic) p 59
[26] Aliotta F, Bellissent-Funel M C, Donato D I, Migliardo P and Vasi C 1992 *Physica* B **180+181** 861
[27] Migliardo P 1993 *J. Mol. Struct.* **296** 229
[28] Bellissent-Funel M C, Dianoux A J, Fontana M P, Maisano G and Migliardo P 1989 *Physica* B **156+157** 132
[29] Bertolini D, Cassettari M, Ferrario M, Salvetti G, Tani A and Grigolini P 1989 *J. Chem. Phys.* **91** 1179
[30] Bermejo F J, Batallan F, Enciso E, White R, Dianoux A J and Howells W S 1990 *J. Phys.: Condens. Matter* **2** 130
[31] Sun S F 1994 *Physical Chemistry of Macromolecules* (New York: Wiley)
[32] Crupi V, Magazù S, Maisano G, Majolino D and Migliardo P 1993 *J. Physique* **5** 6819
[33] Bucaro J A and Litovitz T A 1971 *J. Chem. Phys.* **54** 3846
[34] Gierke T D and Flygare W H J 1974 *Chem. Phys.* **61** 2231
[35] Bertucci S J, Burnham A K, Alms G R and Flygare W H 1988 *J. Chem. Phys.* **66** 605
[36] Aliotta F, Vasi C, Maisano G, Majolino D, Mallamace F and Migliardo P 1986 *J. Chem. Phys.* **84** 4371
[37] Wang C H and Wright R B 1971 *Chem. Phys. Lett.* **11** 277
[38] Keyes T and Kivelson D 1972 *J. Chem. Phys.* **56** 1057
[39] Kivelson D and Madden P 1975 *Mol. Phys.* **30** 1749
[40] Benassi P, Mazzacurati V, Nardone M, Ruocco G and Signorelli G 1989 *J. Chem. Phys.* **91** 6752